Contents lists available at ScienceDirect

Journal of Saudi Chemical Society

journal homepage: www.ksu.edu.sa

Isatin-based ibuprofen and mefenamic acid Schiff base derivatives as dual inhibitors against urease and α–glucosidase: In vitro, *in silico* and cytotoxicity studies

Saima Daud [a], Obaid-ur-Rahman Abid [b], Malik Saadullah [c], M. Fakhar-e-Alam [d], Simone Carradori [e], Asma Sardar [b], Basit Niaz [b], M. Atif [f], Susi Zara [e], Muhammad Rashad [c,e,*]

[a] *Department of Chemistry, Abbottabad University of Science and Technology (AUST), Abbottabad 22500, Pakistan*
[b] *Department of Chemistry, Hazara University, Mansehra 21120, Pakistan*
[c] *Department of Pharmaceutical Chemistry, Government College University Faisalabad, Pakistan*
[d] *Department of Physics, Government College University Faisalabad, Pakistan*
[e] *Department of Pharmacy, "G. d'Annunzio" University of Chieti-Pescara, Via Dei Vestini 31, 66100 Chieti, Italy*
[f] *Department of Physics and Astronomy, College of Science, King Saud University, Riyadh 11541, Saudi Arabia*

ARTICLE INFO

Keywords:
Isatin
NSAIDs derivatives
Multitarget inhibitors (Urease & α-glucosidase)
Molecular docking studies

ABSTRACT

α-Glucosidase and urease inhibitors have emerged as crucial for developing therapeutic drugs targeting diabetes and gastrointestinal disorders. This study reports on new series of ibuprofen and mefenamic acid Schiff base derivatives incorporating isatin as dual inhibitors of α-glucosidase and urease enzymes. These synthesized derivatives (7a-r) were structurally characterized by ^{1}H NMR, ^{13}C NMR and HRMS (EI). Biological evaluation (IC_{50}) identified several derivatives *i.e.,* **7a** (urease = 17.37 ± 1.37 μM, α-glucosidase = 44.1 ± 1.15 μM), **7j**, (urease = 16.61 ± 1.37 μM, α-glucosidase = 81.2 ± 1.33 μM), **7o**, (urease = 18.63 ± 1.27 μM, α-glucosidase = 70.3 ± 1.14 μM), **7r** (urease = 11.36 ± 1.32 μM, α-glucosidase = 39.3 ± 1.17 μM), as dual inhibitors of urease (thiourea 21.37 ± 1.76 μM) and α–glucosidase (acarbose 375.82 ± 1.76 μM) enzymes. These bioactive derivatives were explored for cell viability studies against mononuclear cells revealing a good cytocompatibility. *In silico* molecular docking studies were also conducted to predict the binding mode of new derivatives with target enzymes that were found consistent with the results of *in vitro* research.

1. Introduction

In recent years, the search for novel therapeutic agents with multi-target capabilities has received substantial attention in the realm of drug discovery and development [1,2]. One potential area of research is the discovery of inhibitors targeting enzymes engaged in essential biological processes. Due to their involvement in diseases such as diabetes and gastric problems, α-glucosidase and urease enzymes have emerged as especially enticing targets. α-Glucosidase is an enzyme that hydrolyzes complex carbs into glucose in the small intestine, which directly impacts blood sugar levels [3]. Dysfunction of this enzyme can lead to improper carbohydrate metabolism, contributing to the condition such as diabetes by causing elevated blood sugar levels and impaired glucose hemostasis. The inhibition of this enzyme has been found to successfully manage postprandial hyperglycemia in diabetics [4]. α-Glucosidase inhibitors can modify glucose absorption by decreasing carbohydrate breakdown, leading to better glycemic control [5,6]. As a result, these inhibitors have sparked considerable attention as possible therapeutic agents for the control of diabetes and its consequences [7]. Urease, on the other hand, is an enzyme present in a variety of bacteria (*e.g.*, *H. pylori*), plants as well as the human gastrointestinal mucosa [8]. It catalyzes the hydrolysis of urea into ammonia and carbon dioxide, which is important in bacterial acclimation, growth and in the development of stomach disorders such as peptic ulcers and gastric cancer. Inhibiting urease activity has been identified as a possible therapeutic and preventative method for several disorders [9]. Urease inhibitors can help lower ammonia levels in the stomach, reducing the harmful effects of ammonia on the gastric mucosa. According to the research review, both of these enzymes are now intertwined as the prevalence of *H. pylori* infections among diabetes patients rises as the glycemic index rises [10–12].

* Corresponding author at: Department of Pharmacy, "G. d'Annunzio" University of Chieti-Pescara, Via Dei Vestini 31, 66100 Chieti, Italy.
E-mail address: muhammad.rashad@unich.it (M. Rashad).

https://doi.org/10.1016/j.jscs.2024.101905
Received 17 May 2024; Received in revised form 1 July 2024; Accepted 10 July 2024
Available online 14 July 2024

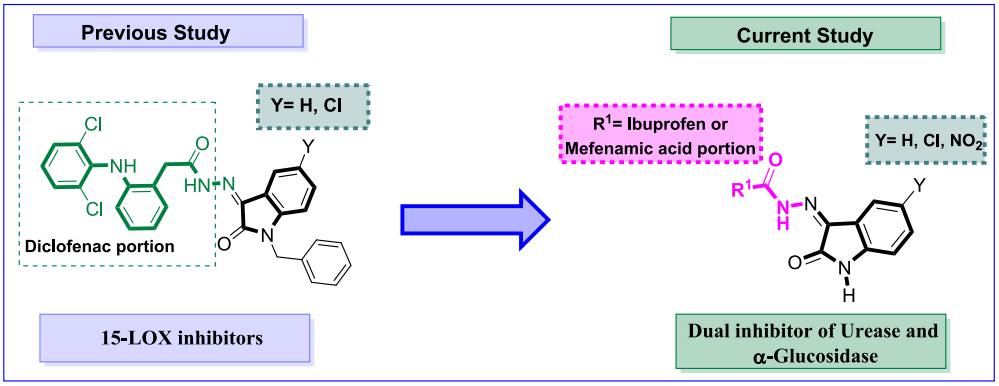

Fig. 1. Rationale of the current study.

Isatin, also known as 1*H*-indole-2,3-dione, has a broad pharmacological range and is hence regarded as a beneficial bioactive heterocyclic moiety [13]. Isatin derivatives exhibit pharmacological activities such as antiproliferative [14–16], antileishmanial [17], antioxidant [18], antimicrobial [19–23], antiplasmodial [24], anti-inflammatory [25], analgesic [26], anticonvulsant [27], anti-urease [28] and anti-α–glucosidase [29] etc., activities. Additionally, Ibuprofen and mefenamic acid are common nonsteroidal anti-inflammatory drugs (NSAIDs) with analgesic, anti-inflammatory, and antipyretic properties [30]. Beyond traditional therapeutic potential, these drugs have demonstrated a variety of other pharmacological activities [31–33], including potential enzyme inhibitory properties [34,35]. By modifying the chemical structures of these drugs [36–43], it is conceivable to integrate new functionalities that selectively target α-glucosidase and urease enzymes [44].

Despite to their well-known biological properties, nonsteroidal anti-inflammatory drugs (NSAIDs) such as ibuprofen and mefenamic acid have not previously been investigated for their possible inhibitory effects on α-glucosidase and urease enzymes. Our research group is leading the way in this effort, to discover new therapeutic compounds that can target both enzymes simultaneously [45–49]. In continuation to our previous work (Fig. 1), we have synthesized derivatives replacing the previously explored naproxen and diclofenac with ibuprofen and mefenamic acid. The goal of this study is to investigate the potential of ibuprofen and mefenamic acid derivatives incorporated with isatin as multitarget inhibitors by methodically introducing structural alterations to improve their inhibitory activity against the two enzymes.

2. Experimental procedure

2.1. Material and methods

All the commercially available reagents and solvents used in this study were purchased from Alfa Aesar and Merck and were utilized without further purification. Bruker FT-300 MHz was used to confirm the structure of the target compounds by ^{1}H NMR and ^{13}C NMR spectra in $CDCl_3$ and DMSO-d_6 as solvents. Chemical shifts were reported in δ part per million (ppm) downfielded from tetramethylsilane (TMS) as the internal standard and the coupling constants were expressed in hertz (Hz). All the reactions were monitored through thin-layer chromatography (TLC) plates precoated with silica gel 60 F_{254}. A Finnegan MAT-311A mass spectrometer was used to record HRMS (EI) spectra. The melting points were obtained (uncorrected) in an open capillary using the Stuart melting point (SMP10) apparatus. The hydrazide of both drugs were synthesized by same procedures as followed by our previous studies [45–48].

2.2. General procedure for the synthesis of N-alkylated isatin intermediates 5(a-f)

A mixture of isatin **4(a,b)** (0.002 mol) and potassium carbonate (0.0025 mol) in DMF (10 mL) was heated in an oil bath at 80 °C for about 30 min. After this, the corresponding alkyl halide (0.0021 mol) was added to the reaction mixture and refluxed for 3–4 h [44]. When the reaction was completed (monitored by TLC), the reaction mixture was poured into ice-water. If the product crystallized, the resulting solid was filtered, washed with water and purified by further recrystallization using ethanol. If not, the suspension was extracted with dichloromethane (DCM) and the organic layer was washed with water, and then dried (over anhydrous sodium sulphate) and concentrated *in vacuo* affording the desired compounds. The detailed spectroscopic analysis of these intermediates (**5a-f**) is provided in the supplementary file.

2.3. General procedure for the synthesis of Schiff base derivatives 7(a-r)

An equimolar mixture of hydrazide **3(a,b)** (1 mmol) and simple isatin **6(a-c)** along with N-alkylated isatin intermediates **5(a-f)** (1 mmol) were refluxed in ethanol (30 mL) in presence of catalytic amount of glacial acetic acid for 2–3 h [46]. After completion of the reaction (checked by TLC), the reaction mixture was allowed to cool and the solid was filtered, washed with water, dried, and recrystallized from ethanol to get pure compounds **7(a-r)**.

2.3.1. 2-(4-isobutylphenyl)-N'-(2-oxoindolin-3-ylidene)propane hydrazide (7a)

Yellowish orange solid; Yield 77 %; R_f = 0.41 (Hex/EtOAc, 4:1); m.p. 188–190 °C; ^{1}H NMR (300 MHz, $CDCl_3$) δ 10.32 (br.s, 1H, NH), 9.89 (br. s, 1H), 7.83 (d, J = 6.7 Hz), 7.65 (dd, J = 7.1, 2.1 Hz), 7.48 (t, J = 7.3 Hz), 7.34 (td, J = 7.1, 2.1 Hz), 7.18 (d, J = 7.8 Hz), 7.03 (d, J = 7.8 Hz, 2H), 3.58 (q, J = 5.3 Hz, 1H), 2.43 (d, J = 8.7 Hz, 2H), 1.90–1.80 (m, 1H), 1.57 (d, J = 5.3 Hz, 3H), 0.84 (d, J = 5.0 Hz, 6H). ^{13}C NMR (75 MHz, $CDCl_3$) δ 170.3, 167.5, 143.1, 139.5, 139.5, 138.4, 129.3, 128.4, 124.4, 123.1, 122.0, 121.1, 112.6, 45.5, 43.7, 26.9, 22.6, 18.2. HRMS (EI) calcd for $C_{21}H_{23}N_3O_2$ [M^+]: 349.1790, found 349.1782.

2.3.2. 2-(4-isobutylphenyl)-N'-(2-oxo-1-propylindolin-3-ylidene)propane hydrazide (7b)

Yellow semisolid/oil; R_f = 0.56 (Hex/EtOAc, 4:1); Yield 78 %. ^{1}H NMR (300 MHz, $CDCl_3$) δ 9.99 (br.s, 1H), 7.83 (d, J = 6.6 Hz, 1H), 7.65 (d, J = 6.3 Hz, 1H), 7.46 (t, J = 6.8 Hz, 1H), 7.27 (t, J = 6.9 Hz, 1H), 7.18 (d, J = 7.8 Hz, 2H), 7.03 (d, J = 7.8 Hz, 2H), 4.29 (t, J = 7.4 Hz, 2H), 3.63 (q, J = 5.4 Hz, 1H), 2.43 (d, J = 8.8 Hz, 2H), 1.91–1.76 (m, 3H), 1.55 (d, J = 5.4 Hz, 3H), 1.07 (t, J = 5.3 Hz, 3H), 0.86 (d, J = 5.0 Hz, 6H). ^{13}C NMR (75 MHz, $CDCl_3$) δ 170.4, 163.4, 143.1, 139.8, 138.5, 138.4, 130.4, 129.3, 124.3, 123.6, 122.2, 121.5, 112.8, 46.3, 45.6, 43.7, 26.9, 23.4, 22.5, 18.1, 11.4. HRMS (EI) calcd for $C_{24}H_{29}N_3O_2$ [M^+]:

391.2260, found 391.2252.

2.3.3. N'-(1-benzyl-2-oxoindolin-3-ylidene)-2-(4-isobutylphenyl)propane hydrazide (7c)

Yellow sticky semisolid; Yield 80 %. $R_f = 0.58$ (Hex/EtOAc, 4:1). ^{1}H NMR (300 MHz, $CDCl_3$) δ 10.09 (br. s, 1H), 7.83 (d, $J = 6.6$ Hz, 1H), 7.65 (d, $J = 7.5$ Hz, 1H), 7.46 (t, $J = 6.9$ Hz, 1H), 7.32–7.22 (m, 6H), 7.16 (d, $J = 7.8$ Hz, 2H), 7.02 (d, $J = 7.8$ Hz, 2H), 4.93 (s, 2H), 3.58 (q, $J = 5.4$ Hz, 1H), 2.41 (d, $J = 8.7$ Hz, 2H), 1.89–1.80 (m, 1H), 1.56 (d, $J = 7.2$ Hz, 3H), 0.88 (d, $J = 6.0$ Hz, 6H). ^{13}C NMR (75 MHz, $CDCl_3$) δ 170.3, 165.9, 143.1, 139.8, 138.5, 138.4, 136.7, 130.3, 129.3, 128.5, 127.6, 127.4, 124.3, 122.9, 122.2, 121.7, 112.7, 45.5, 45.4, 43.7, 26.9, 22.4, 18.1. HRMS (EI) calcd for $C_{28}H_{29}N_3O_2$ [M^+]: 439.2260, found 439.2253.

2.3.4. N'-(1-butyl-2-oxoindolin-3-ylidene)-2-(4-isobutylphenyl)propane hydrazide (7d)

Yellowish sticky semisolid; Yield 77 %. $R_f = 0.58$ (Hex/EtOAc, 4:1). ^{1}H NMR (300 MHz, $CDCl_3$) δ 10.06 (br. s, 1H), 7.83 (d, $J = 6.6$ Hz, 1H), 7.65 (d, $J = 6.3$ Hz, 1H), 7.46 (t, $J = 6.7$ Hz, 1H), 7.27 (t, $J = 6.9$ Hz, 1H,), 7.18 (d, $J = 7.8$ Hz, 2H), 7.09 (d, $J = 7.8$ Hz, 2H), 4.59 (t, $J = 9.1$ Hz, 2H), 3.58 (q, $J = 5.4$ Hz, 1H), 2.49 (d, $J = 8.7$ Hz, 2H), 2.17 (quin, $J = 8.7$ Hz, 2H), 1.90–1.80 (m, 1H), 1.57 (d, $J = 5.4$ Hz, 3H), 1.45–1.33 (m, 2H), 1.04 (t, $J = 4.8$ Hz, 3H), 0.91 (d, $J = 4.9$ Hz, 6H). ^{13}C NMR (75 MHz, $CDCl_3$) δ 170.1, 163.4, 143.3, 139.8, 138.5, 138.4, 130.4, 129.3, 124.3, 123.5, 122.1, 121.5, 112.8, 46.8, 45.3, 43.5, 29.3, 26.9, 22.6, 19.4, 18.0, 13.6. HRMS (EI) calcd for $C_{25}H_{31}N_3O_2$ [M^+]: 405.2416, found 405.2409.

2.3.5. N'-(1-allyl-2-oxoindolin-3-ylidene)-2-(4-isobutylphenyl)propane hydrazide (7e)

Brick red solid; Yield 73 %; $R_f = 0.49$ (Hex/EtOAc, 4:1); m.p. 105–108 °C. ^{1}H NMR (300 MHz, $CDCl_3$) δ 10.14 (br. s, 1H), 7.83 (d, $J = 6.6$ Hz, 1H), 7.65 (d, $J = 7.8$ Hz, 1H), 7.46 (t, $J = 6.9$ Hz, 1H), 7.29 (t, $J = 6.9$ Hz, 1H), 7.18 (d, $J = 7.8$ Hz, 2H), 7.02 (d, $J = 7.8$ Hz, 2H), 5.99 – 5.87 (m, 1H), 5.18 (d, $J = 8.4$ Hz, 2H), 4.90 (d, $J = 7.8$ Hz, 2H), 3.58 (q, $J = 5.4$ Hz, 1H), 2.56 (d, $J = 8.7$ Hz, 2H), 1.89–1.80 (m, 1H), 1.57 (d, $J = 5.4$ Hz, 3H), 0.88 (d, $J = 5.7$ Hz, 6H). ^{13}C NMR (75 MHz, $CDCl_3$) δ 170.3, 162.1, 143.1, 140.8, 138.5, 137.7, 133.5, 130.3, 129.4, 124.3, 123.2, 122.1, 121.7, 117.7, 112.85, 46.0, 43.5, 38.4, 26.9, 22.4, 18.1. HRMS (EI) calcd for $C_{24}H_{27}N_3O_2$ [M^+]: 389.2103, found 389.2095.

2.3.6. N'-(5-chloro-2-oxoindolin-3-ylidene)-2-(4-isobutylphenyl)propane hydrazide (7f)

Shiny yellow crystalline solid; Yield 73 %. $R_f = 0.48$ (Hex/EtOAc, 4:1); m.p. 112–114 °C. ^{1}H NMR (300 MHz, $CDCl_3$) δ 10.26 (br. s, 1H), 10.02 (br. s, 1H), 7.73 (d, $J = 1.6$ Hz, 1H), 7.61 (dd, $J = 7.4$, 2.0 Hz, 1H), 7.45 (d, $J = 7.4$ Hz, 1H), 7.18 (d, $J = 7.8$ Hz, 2H), 7.04 (d, $J = 7.8$ Hz, 2H), 3.58 (q, $J = 5.4$ Hz, 1H), 2.42 (d, $J = 8.7$ Hz, 2H), 1.90–1.80 (m, 1H), 1.57 (d, $J = 5.4$ Hz, 3H), 0.89 (d, $J = 5.0$ Hz, 6H). ^{13}C NMR (75 MHz, $CDCl_3$) δ 170.1, 167.5, 143.1, 139.1, 138.4, 138.4, 130.4, 129.3, 127.3, 124.3, 122.7, 121.8, 114.4, 45.5, 43.7, 26.9, 22.4, 18.1. HRMS (EI) calcd for $C_{21}H_{22}ClN_3O_2$ [M^+]: 383.1401, found 383.1394.

2.3.7. N'-(5-chloro-2-oxo-1-propylindolin-3-ylidene)-2-(4-isobutylphenyl) propane hydrazide (7g)

Brown oil; Yield 84 %; $R_f = 0.59$ (Hex/EtOAc, 4:1). ^{1}H NMR (300 MHz, $CDCl_3$) δ 10.14 (br.s, 1H), 7.61–7.56 (m, 2H), 7.45 (dd, $J = 8.0$, 2.1 Hz, 1H), 7.18 (d, $J = 7.8$ Hz, 2H), 7.01 (d, $J = 7.8$ Hz, 2H), 4.15 (t, $J = 7.8$ Hz, 2H), 3.58 (q, $J = 5.4$ Hz, 1H), 2.50 (d, $J = 8.7$ Hz, 2H), 1.90–1.73 (m, 3H), 1.57 (d, $J = 5.4$ Hz, 3H), 1.00 (t, $J = 5.2$ Hz, 3H), 0.89 (d, $J = 4.9$ Hz, 6H). ^{13}C NMR (75 MHz, $CDCl_3$) δ 170.2, 163.4, 143.1, 138.9, 138.4, 138.1, 129.3, 129.3, 127.3, 124.3, 122.6, 122.1, 113.2, 46.3, 45.5, 43.7, 26.9, 23.4, 22.6, 18.2, 11.41. HRMS (EI) calcd for $C_{24}H_{28}ClN_3O_2$ [M^+]: 425.1870, found 425.1862.

2.3.8. N'-(1-benzyl-5-chloro-2-oxoindolin-3-ylidene)-2-(4-isobutylphenyl) propane hydrazide (7h)

Yellow solid; Yield 79 %; $R_f = 0.60$ (Hex/EtOAc, 4:1); m.p. 88–90 °C. ^{1}H NMR (300 MHz, $CDCl_3$) δ 10.17 (br.s, 1H), 7.73 (d, $J = 1.9$ Hz, 1H), 7.64 (dd, $J = 8.0$, 1.8 Hz, 1H), 7.53 (d, $J = 8.1$ Hz, 1H), 7.41–7.27 (m, 5H), 7.18 (d, $J = 7.8$ Hz, 2H), 7.00 (d, $J = 7.8$ Hz, 2H), 4.90 (s, 2H), 3.58 (q, $J = 5.4$ Hz, 1H), 2.47 (d, $J = 8.6$ Hz, 2H), 1.90–1.80 (m, 1H), 1.57 (d, $J = 5.4$ Hz, 3H), 0.90 (d, $J = 5.0$ Hz, 6H). ^{13}C NMR (75 MHz, $CDCl_3$) δ 170.4, 165.9, 143.1, 139.0, 138.4, 138.0, 136.7, 129.3, 129.3, 128.5, 127.6, 127.4, 124.3, 122.5, 121.9, 113.2, 45.7, 45.4, 43.7, 26.9, 22.6, 18.1. HRMS (EI) calcd for $C_{28}H_{28}ClN_3O_2$ [M^+]: 473.1870, found 473.1863.

2.3.9. 2-(4-isobutylphenyl)-N'-(5-nitro-2-oxoindolin-3-ylidene)propane hydrazide (7i)

Yellow solid; Yield 61 %; $R_f = 0.50$ (Hex/EtOAc, 4:1); m.p. 90–95 °C. ^{1}H NMR (300 MHz, $CDCl_3$) δ 10.50 (br.s, 1H), 10.00 (br.s, 1H), 8.05 (d, $J = 1.8$ Hz, 1H), 7.88 (dd, $J = 7.5$, 1.8 Hz, 1H), 7.61 (d, $J = 7.8$ Hz, 1H), 7.18 (d, $J = 7.8$ Hz, 2H), 7.02 (d, $J = 7.8$ Hz, 2H), 3.58 (q, $J = 5.4$ Hz, 1H), 2.42 (d, $J = 8.7$ Hz, 2H), 1.89–1.80 (m, 1H), 1.56 (d, $J = 7.2$ Hz, 3H), 0.88 (d, $J = 7.2$ Hz, 6H). ^{13}C NMR (75 MHz, $CDCl_3$) δ 170.5, 167.5, 143.1, 142.0, 141.4, 139.1, 138.4, 129.3, 129.0, 124.3, 120.6, 119.1, 112.9, 45.5, 43.7, 26.9, 22.4, 18.1. HRMS (EI) calcd for $C_{21}H_{22}N_4O_4$ [M^+]: 394.1641, found 349.1633.

2.3.10. 2-((2,3-dimethylphenyl)amino)-N'-(2-oxoindolin-3-ylidene)benzo hydrazide (7j)

Yellow solid; Yield 78 %. $R_f = 0.47$ (Hex/EtOAc, 4:1); m.p. 244–245 °C. ^{1}H NMR (300 MHz, $CDCl_3$) δ 10.10 (br. s, 1H), 9.57 (s, 1H), 8.11 (s, 1H), 7.89–7.82 (m, 2H), 7.65 (dd, $J = 7.4$, 2.1 Hz, 1H), 7.46 (t, $J = 7.3$ Hz, 1H), 7.30–7.06 (m, 5H), 6.92 (d, $J = 7.5$ Hz, 1H), 6.58 (d, $J = 7.8$ Hz, 1H), 2.28 (s, 3H), 2.13 (s, 3H). ^{13}C NMR (75 MHz, $CDCl_3$) δ 169.7, 167.5, 144.7, 143.2, 139.3, 137.6, 136.7, 129.7, 129.5, 128.4, 127.8, 127.3, 127.1, 123.0, 122.0, 121.1, 120.8, 119.9, 118.3, 112.6, 20.3, 12.8. HRMS (EI) calcd for $C_{23}H_{20}N_4O_2$ [M^+]: 384.1586, found 384.1578.

2.3.11. 2-((2,3-dimethylphenyl)amino)-N'-(2-oxo-1-propylindolin-3-ylidene)benzo hydrazide (7k)

Reddish orange solid; Yield 79 %. $R_f = 0.57$ (Hex/EtOAc, 4:1); m.p. 174–176 °C. ^{1}H NMR (300 MHz, DMSO-d_6) δ 10.47 (br.s, 1H), 8.78 (s, 1H), 8.03 (d, $J = 8.2$ Hz, 1H), 7.92 (d, $J = 7.6$ Hz, 1H), 7.79 (d, $J = 8.2$ Hz, 1H), 7.69–7.34 (m, 2H), 7.35–7.27 (m, 2H), 7.12–7.02 (m, 2H), 6.92 (d, $J = 7.6$ Hz, 1H), 6.53 (d, $J = 7.7$ Hz, 1H), 4.28 (t, $J = 7.4$ Hz, 2H), 2.28 (s, 3H), 2.12 (s, 3H), 1.75–1.65 (m, 2H), 1.00 (t, $J = 5.2$ Hz, 3H). ^{13}C NMR (75 MHz, DMSO-d_6) δ 169.0, 163.5, 144.3, 143.2, 139.9, 137.4, 136.0, 130.0, 129.4, 129.3, 127.7, 127.3, 127.0, 123.5, 122.1, 122.0, 121.5, 120.8, 119.9, 118.3, 112.5, 46.6, 23.9, 20.6, 12.1, 11.4. HRMS (EI) calcd for $C_{26}H_{26}N_4O_2$ [M^+]: 426.2056, found 426.2048.

2.3.12. N'-(1-benzyl-2-oxoindolin-3-ylidene)-2-((2,3-dimethylphenyl) amino)benzo hydrazide (7l)

Dark brown solid; Yield 66 %. $R_f = 0.57$ (Hex/EtOAc, 4:1); m.p. 216–218 °C. ^{1}H NMR (300 MHz, DMSO-d_6) δ 10.47 (br.s, 1H), 8.58 (s, 1H), 8.15 (d, $J = 7.8$ Hz, 1H), 7.92 (d, $J = 6.7$ Hz, 1H), 7.79 (d, $J = 8.2$ Hz, 1H), 7.70–7.63 (m, 2H), 7.40–7.20 (m, 7H), 7.12–7.02 (m, 2H), 6.92 (d, $J = 7.6$ Hz, 1H), 6.53 (d, $J = 7.7$ Hz, 1H), 4.94 (s, 2H), 2.28 (s, 3H), 2.12 (s, 3H). ^{13}C NMR (75 MHz, DMSO-d_6) δ 169.0, 165.9, 144.1, 143.0, 139.8, 137.1, 136.8, 136.7, 130.3, 129.7, 129.5, 128.5, 127.9, 127.6, 127.4, 127.3, 127.0, 122.9, 122.2, 122.0, 121.7, 120.8, 119.1, 118.4, 112.7, 45.3, 20.1, 12.6. HRMS (EI) calcd for $C_{30}H_{26}N_4O_2$ [M^+]: 474.2056, found 474.2049.

2.3.13. N'-(1-butyl-2-oxoindolin-3-ylidene)-2-((2,3-dimethylphenyl) amino)benzo hydrazide (7m)

Orange solid; Yield 79 %. $R_f = 0.61$ (Hex/EtOAc, 4:1); m.p.

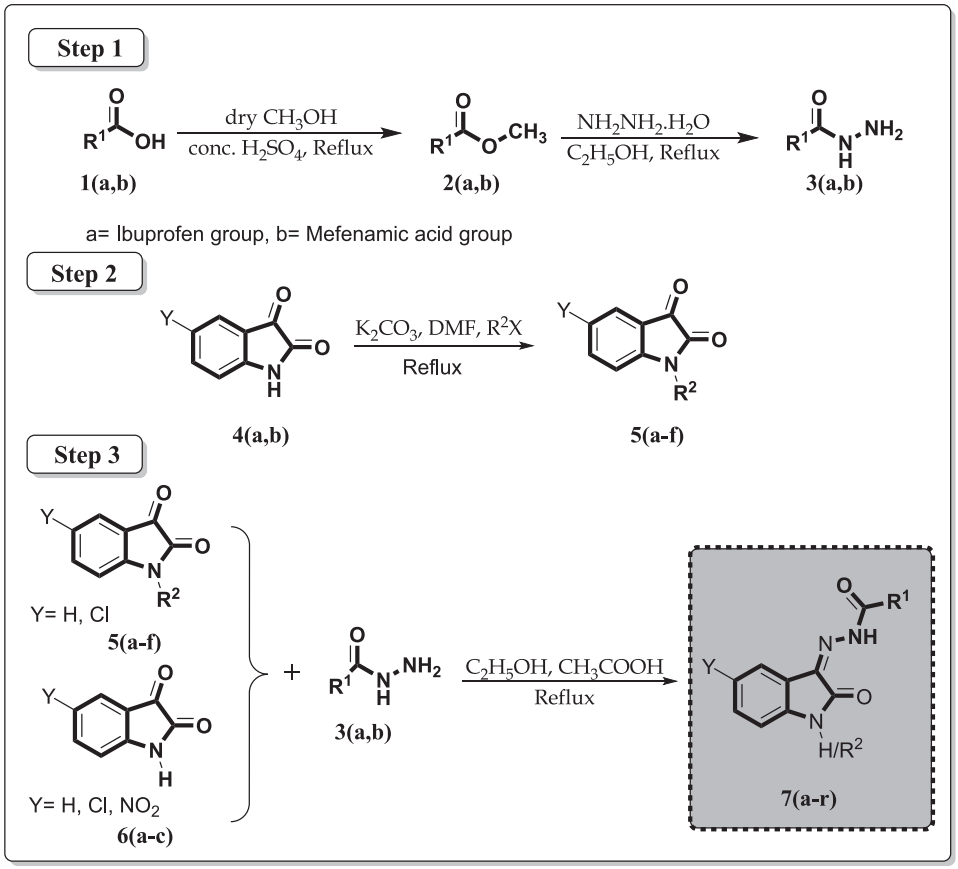

Scheme 1. Synthetic route to isatin substituted Schiff base derivatives of ibuprofen and mefenamic acid.

163–165 °C. ^{1}H NMR (300 MHz, DMSO-d_6) δ 10.41 (br.s, 1H), 8.79 (br. s, 1H), 7.97 (d, J = 8.1 Hz, 1H), 7.92 (dd, J = 6.0, 1.8 Hz, 1H), 7.79 (d, J = 8.4 Hz, 1H), 7.68–7.63 (m, 2H), 7.35–7.27 (m, 2H), 7.10–7.02 (m, 2H), 6.90 (d, J = 7.5 Hz, 1H), 6.53 (d, J = 7.8 Hz, 1H), 4.34 (t, J = 8.4 Hz, 2H), 2.28 (s, 3H), 2.12 (s, 3H), 1.64–1.40 (m, 4H), 0.91 (t, J = 4.8 Hz, 3H). ^{13}C NMR (75 MHz, DMSO-d_6) δ 168.7, 163.4, 144.7, 143.2, 139.8, 137.1, 136.6, 130.4, 129.7, 129.5, 127.7, 127.3, 127.1, 123.5, 122.1, 122.0, 121.5, 120.7, 119.6, 118.3, 112.8, 46.8, 29.3, 20.3, 19.4, 13.6, 12.8. HRMS (EI) calcd for $C_{27}H_{28}N_4O_2$ [M^+]: 470.2212, found 470.2204.

2.3.14. *N'-(1-allyl-2-oxoindolin-3-ylidene)-2-((2,3-dimethylphenyl) amino)benzo hydrazide (7n)*

Orange solid; Yield 72 %; R_f = 0.58 (Hex/EtOAc, 4:1); m.p. 206–209 °C. ^{1}H NMR (300 MHz, DMSO-d_6) δ 10.55 (br.s, 1H), 8.75 (s, 1H), 8.07 (d, J = 7.7 Hz, 1H), 7.92 (d, J = 7.8 Hz, 1H), 7.79 (d, J = 7.8 Hz, 1H), 7.66–7.63 (m, 2H), 7.35–7.27 (m, 2H), 7.12–7.02 (m, 2H), 6.92 (d, J = 7.6 Hz, 1H), 6.50 (d, J = 7.7 Hz, 1H), 6.01–5.85 (m, 1H), 5.16 (d, J = 16.2 Hz, 2H), 4.90 (d, J = 7.7 Hz, 2H), 2.28 (s, 3H), 2.12 (s, 3H). ^{13}C NMR (75 MHz, DMSO-d_6) δ 167.5, 163.8, 145.3, 143.0, 139.7, 137.1, 136.7, 133.6, 130.3, 129.7, 129.5, 127.7, 127.3, 127.1, 123.3, 122.1, 122.0, 121.6, 120.8, 118.4, 118.3, 117.7, 112.8, 39.5, 20.0, 12.3. HRMS (EI) calcd for $C_{26}H_{24}N_4O_2$ [M^+]: 424.1899, found 424.1891.

2.3.15. *N'-(5-chloro-2-oxoindolin-3-ylidene)-2-((2,3-dimethylphenyl) amino)benzo hydrazide (7o)*

Yellowish orange solid; Yield 58 %. R_f = 0.49 (Hex/EtOAc, 4:1); m.p. 172–174 °C. ^{1}H NMR (300 MHz, DMSO-d_6) δ 10.71 (br.s, 1H), 10.03 (s, 1H), 8.61 (s, 1H), 8.15 (d, J = 8.0 Hz, 1H), 8.00 (d, J = 2.0 Hz, 1H), 7.75–7.61 (m, 3H), 7.45 (dd, J = 7.5, 2.0 Hz, 1H), 7.11–7.02 (m, 2H), 6.92 (d, J = 7.5 Hz, 1H), 6.50 (d, J = 7.8 Hz, 1H), 2.28 (s, 3H), 2.12 (s, 3H). ^{13}C NMR (75 MHz, DMSO-d_6) δ 169.2, 167.5, 144.0, 143.2, 138.7, 137.1, 136.7, 130.4, 129.7, 129.5, 127.7, 127.4, 127.1, 122.7, 122.0, 121.8, 120.8, 119.7, 118.3, 114.4, 20.3, 12.8. HRMS (EI) calcd for $C_{23}H_{19}ClN_4O_2$ [M^+]: 418.1197, found 418.1189.

2.3.16. *N'-(5-chloro-2-oxo-1-propylindolin-3-ylidene)-2-((2,3-dimethylphenyl)amino)benzo hydrazide (7p)*

Shiny orange solid; Yield 83 %. R_f = 0.65 (Hex/EtOAc, 4:1); m.p. 180–183 °C. ^{1}H NMR (300 MHz, DMSO-d_6) δ 10.44 (s, 1H), 8.50 (s, 1H), 8.08 (dd, J = 7.8, 1.2 Hz, 1H), 7.82 (d, J = 1.8 Hz, 1H), 7.59–7.43 (m, 3H), 7.25 (dd, J = 7.8, 1.8 Hz, 1H), 7.10–7.02 (m, 2H), 6.91 (d, J = 7.8 Hz, 1H), 6.52 (d, J = 7.8 Hz, 1H), 4.28 (t, J = 7.5 Hz, 2H), 2.28 (s, 3H), 2.12 (s, 3H), 1.75–1.64 (m, 2H), 1.00 (t, J = 5.1 Hz, 3H). ^{13}C NMR (75 MHz, DMSO-d_6) δ 169.7, 163.4, 144.7, 143.2, 138.9, 136.7, 136.6, 129.7, 129.5, 129.3, 127.7, 127.4, 127.3, 127.1, 122.6, 122.1, 122.0, 120.7, 119.9, 118.3, 113.2, 46.3, 23.4, 20.3, 12.8, 11.4. HRMS (EI) calcd for $C_{26}H_{25}ClN_4O_2$ [M^+]: 460.1666, found 460.1658.

2.3.17. *N'-(1-benzyl-5-chloro-2-oxoindolin-3-ylidene)-2-((2,3-dimethylphenyl) amino)benzo hydrazide (7q)*

Orange solid; Yield 79 %. R_f = 0.69 (Hex/EtOAc, 4:1); m.p. 229–231 °C. ^{1}H NMR (300 MHz, DMSO-d_6) δ 10.49 (br.s, 1H), 8.72 (s, 1H), 8.03 (d, J = 2.0 Hz, 1H), 7.89 (dd, J = 7.9, 2.0 Hz, 1H), 7.77 (d, J = 8.3 Hz, 1H), 7.69–7.61 (m, 2H), 7.47 (d, J = 8.2 Hz, 1H), 7.32–7.26 (m, 5H), 7.12–7.02 (m, 2H), 6.92 (d, J = 7.6 Hz, 1H), 6.49 (d, J = 7.8 Hz, 1H), 4.94 (s, 2H), 2.28 (s, 3H), 2.12 (s, 3H). ^{13}C NMR (75 MHz, DMSO-d_6) δ 169.5, 165.9, 144.1, 143.0, 139.0, 136.8, 136.7, 136.0, 129.7, 129.5, 129.3, 128.5, 127.7, 127.6, 127.4, 127.3, 127.1, 122.5, 122.0, 121.9, 120.8, 119.4, 118.3, 113.2, 45.4, 20.3, 12.1. HRMS (EI) calcd for $C_{30}H_{25}ClN_4O_2$ [M^+]: 508.1666, found 508.1659.

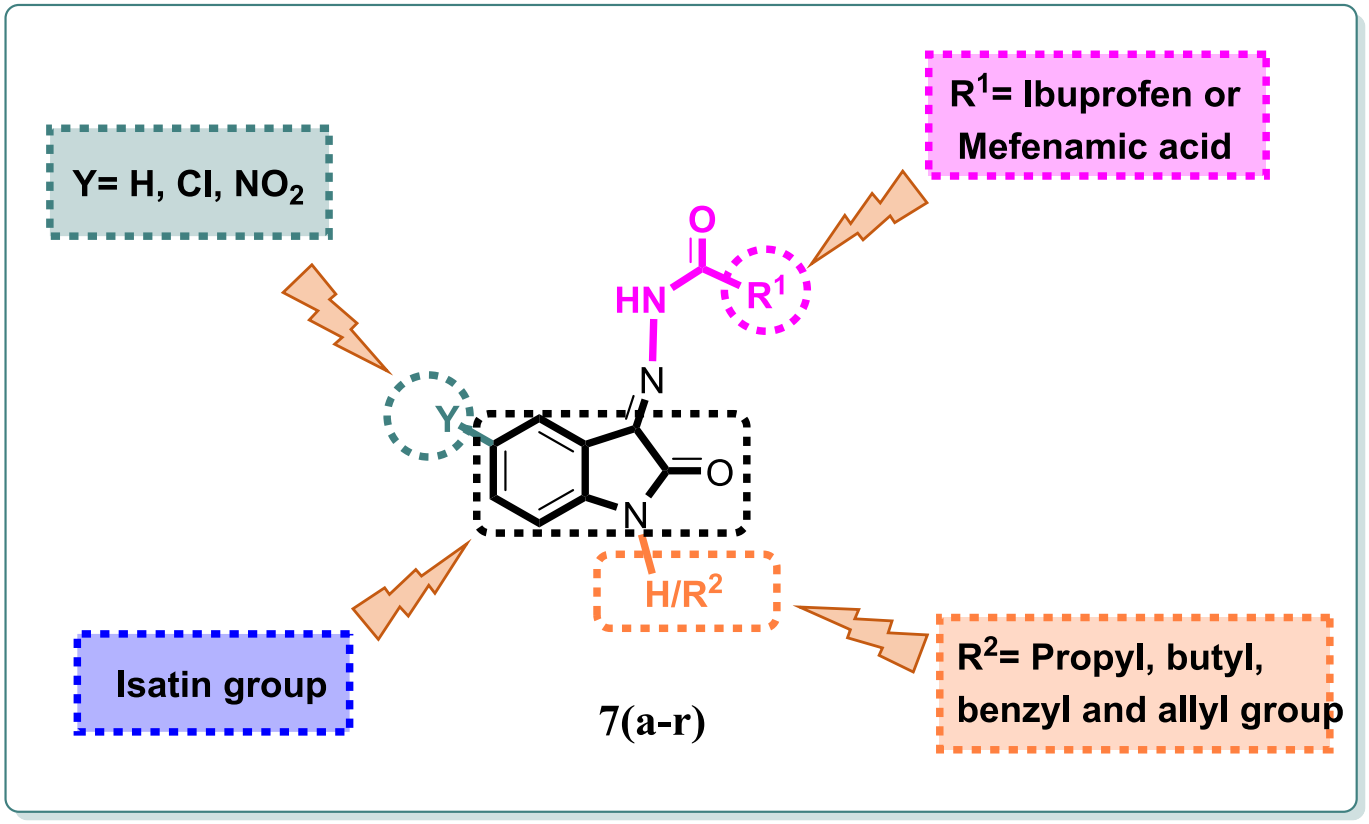

Fig. 2. General structural features of isatin substituted Schiff base derivatives.

2.3.18. 2-((2,3-dimethylphenyl)amino)-N'-(5-nitro-2-oxoindolin-3-ylidene)benzo hydrazide (7r)

Orange solid; Yield 68 %. R_f = 0.62 (Hex/EtOAc, 4:1); m.p. 232–235 °C. ^{1}H NMR (300 MHz, DMSO-d_6) δ 10.49 (br.s, 1H), 9.44 (s, 1H), 8.63 (s, 1H), 8.20 (d, J = 1.8 Hz, 1H), 7.87 (dd, J = 7.6, 2.0 Hz, 1H), 7.67 (d, J = 7.7 Hz, 1H), 7.42–7.28 (m, 3H), 7.12–7.02 (m, 2H), 6.92 (d, J = 7.5 Hz, 1H), 6.54 (d, J = 7.7 Hz, 1H), 2.28 (s, 3H), 2.12 (s, 3H). ^{13}C NMR (75 MHz, DMSO-d_6) δ 170.0, 167.5, 144.4, 143.3, 141.8, 141.4, 137.1, 136.7, 129.7, 129.5, 129.0, 127.6, 127.4, 127.0, 122.0, 120.8, 120.6, 119.7, 119.1, 118.3, 112.9, 20.5, 12.9. HRMS (EI) calcd for $C_{23}H_{19}N_5O_2$ [M^+]: 429.1437, found 429.1430.

2.4. Biological evaluation

All the synthesized derivatives were biologically evaluated for *in vitro* urease, α-glucosidase inhibitory potential, as well as cell viability studies [45,50–52]. The procedure used for these activities and rationale for enzyme selection are provided in supplementary file.

2.5. Docking methodology

To predict the mechanism of inhibition and binding mode of the synthesized compounds, a molecular operating environment (MOE) software was used to dock the most active compounds with the active sites of the target enzymes [53,54]. As the crystal structure of α-glucosidase is still unknown, we utilized the homology model provided by Liu et al [55], and the urease (PDB ID: 4ubp) [56] was obtained from the Protein Data Bank (PDB). The 3D structures of isolated molecules were constructed after the elimination of water molecules, using the builder tool in MOE program. Using the MOE's default parameters (Force Field: MMFF94X gradient: 0.05), it was revealed that the active compounds were energy minimized and 3D protonated. The 3D structures of most potent derivatives were also generated in MOE and the energy was minimized using the MOE's default parameters. Both α-glucosidase and urease were docked to the compounds using MOE's default parameters, which were Placement: Triangle Matcher, Refinement: Induced Fit, and Rescoring: London dG. Ten conformations were created for each ligand. Each compound's top-ranked conformation was utilized for further investigation. Following molecular docking, the best poses were analyzed using Discovery Studio software.

Table 1
Different substituents of Schiff base derivatives 7(a-r).

Compd.	R^1	R^2	Y	Compd.	R^1	R^2	Y
7a	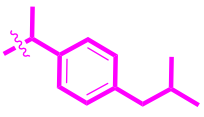	H	H	7j		H	H
7b		$CH_2CH_2CH_3$	H	7k		$CH_2CH_2CH_3$	H
7c		$CH_2C_6H_5$	H	7l		$CH_2C_6H_5$	H
7d		$CH_2CH_2CH_2CH_3$	H	7*m*		$CH_2CH_2CH_2CH_3$	H
7e		$CH_2CH=CH_2$	H	7*n*		$CH_2CH=CH_2$	H
7f		H	Cl	7o		H	Cl
7g		$CH_2CH_2CH_3$	Cl	7p		$CH_2CH_2CH_3$	Cl
7h		$CH_2C_6H_5$	Cl	7q		$CH_2C_6H_5$	Cl
7i		H	NO_2	7r		H	NO_2

Table 2
In vitro urease and α-glucosidase inhibition activity and cell viability of Isatin Schiff base derivatives **7(a-r)**.

Compound	Urease inhibition IC_{50} (μM)	α-Glucosidase inhibition IC_{50} (μM)	Cell viability (%) at 0.25 mM
7a	17.37 ± 1.37	44.1 ± 1.15	69.5 ± 1.7
7b	20.56 ± 1.49	na	60.7 ± 1.3
7c	36.52 ± 1.33	131.1 ± 1.10	66.4 ± 1.5
7d	33.56 ± 1.52	28.2 ± 1.62	55.3 ± 1.4
7e	60.49 ± 1.53	na	31.2 ± 1.2
7f	39.18 ± 1.84	397.5 ± 1.12	41.3 ± 1.7
7g	45.63 ± 1.73	49.2 ± 1.31	59.7 ± 1.4
7h	68.28 ± 1.16	445.3 ± 2.32	36.8 ± 1.2
7i	13.38 ± 1.75	441.3 ± 1.11	78.9 ± 1.6
7j	16.61 ± 1.37	81.2 ± 1.33	72.5 ± 1.4
7k	59.37 ± 1.59	66.4 ± 1.41	62.3 ± 1.9
7l	41.17 ± 1.39	97.2 ± 1.19	67.6 ± 1.6
7*m*	71.25 ± 1.41	73.1 ± 1.16	54.5 ± 1.4
7*n*	76.51 ± 1.48	na	47.4 ± 1.3
7o	18.63 ± 1.27	70.3 ± 1.14	95.9 ± 1.5
7p	53.18 ± 1.37	60.5 ± 1.53	76.7 ± 1.7
7q	66.83 ± 1.66	55.4 ± 1.41	77.5 ± 1.3
7r	11.36 ± 1.32	39.3 ± 1.17	79.6 ± 1.5
Thiourea	21.37 ± 1.76	–	91.6 ± 1.4
Acarbose	–	375.8 ± 1.76	–
Cyclophosphamide	–	–	56.5 ± 1.8
Cisplatin	–	–	51.7 ± 1.9
Curcumin	–	–	73.9 ± 1.7

na: not active at the highest concentration tested (0.25 mM).

3. Result and discussions

3.1. Chemistry

The synthesis of isatin substituted ibuprofen and mefenamic acid Schiff base derivatives **7(a-r)** was achieved through a three-step reaction in good yields. Scheme 1 showed the original synthetic route to prepare final Schiff bases, starting from the acid form of both drugs. The substituents are illustrated and displayed in Fig. 2 and Table 1, respectively. In this study we first synthesized ibuprofen and mefenamic hydrazide derivatives **3(a,b)** followed by the synthesis of their ester counterparts as described in our earlier study [45]. In the second step, we synthesized six different N-alkylated intermediates of simple and substituted isatin **5 (a-f)**. The synthesis of these analogs was confirmed through their ^{1}H NMR spectra which showed the emergence of aliphatic chain protons in the range of 5.93–1.00 ppm, while the aromatic protons appear at 8.09–7.07 ppm. The investigation of ^{13}C NMR also confirmed the formation of these N-alkylated isatin intermediates. In the last step, the N-alkylated **5(a-f)** and non-alkylated **6(a-c)** analogs reacted with hydrazide of both drugs to form isatin substituted Schiff base derivatives of ibuprofen and mefenamic acid **7(a-r)** (Table 1). The synthesized Schiff base derivatives **7(a-r)** were characterized by their ^{1}H NMR and ^{13}C NMR spectral data. In ^{1}H NMR spectra, the amidic NH appears between 10.71–10.06 ppm. The free NH protons of isatin moiety in case of **7a**, **7f**, **7i**, **7j**, **7o** and **7r** resonate between 10.03–9.44 ppm, while in case of mefenamic acid derivatives **7(j-r)**, the NH protons are between 8.79–8.11 ppm. Allylic CH and CH_2 protons in the case of **7e** and **7n** were found between 6.01–5.16 ppm. The aliphatic protons have shown signals at 4.94–0.84 ppm, while the aromatic protons signals were found in 8.20–6.49 ppm range. In ^{13}C NMR spectra, the absence of C = O signal and formation of the characteristic signal of the imine carbon (−C = N) was observed between 140.87–136.72 ppm. The HRMS analysis of these derivatives also supported the synthesis and purity by showing molecular ion peak M^+ at *m/z* in their respective regions.

3.2. Biological evaluation

3.2.1. Urease inhibition and Structure-Activity relationship (SAR) studies

The isatin Schiff base derivatives **7(a-r)** were screened for their jack bean urease inhibition according to the literature protocol [57]. All compounds demonstrated inhibitory potential with IC_{50} value between 76.51 ± 1.48 μM to 11.36 ± 1.32 μM, whereas the standard thiourea has an IC_{50} value of 21.37 ± 1.76 μM, respectively. Among the synthetic library, compounds **7a** (IC_{50} = 17.37 ± 1.37 μM), **7b** (IC_{50} = 20.56 ± 1.49 μM), **7i** (IC_{50} = 13.38 ± 1.75 μM), **7j** (IC_{50} = 16.61 ± 1.37 μM), **7o** (IC_{50} = 18.63 ± 1.27 μM), and **7r** (IC_{50} = 11.36 ± 1.32 μM) emerged to be the potent inhibitors with IC_{50}s lower than the standard thiourea. Conversely, compounds **7c**, **7d**, **7f**, **7g**, and **7l** with IC_{50} values of 36.52 ± 1.33 μM, 33.56 ± 1.52 μM, 39.18 ± 1.84 μM, 45.63 ± 1.73 μM, 41.17 ± 1.39 μM were found as moderate inhibitors for urease enzyme. Finally, compounds **7e** (IC_{50} = 60.49 ± 1.53 μM), **7h** (IC_{50} = 68.28 ± 1.16 μM), **7k** (IC_{50} = 59.37 ± 1.59 μM), **7m** (IC_{50} = 71.25 ± 1.41 μM), **7n** (IC_{50} = 76.51 ± 1.48 μM), **7p** (IC_{50} = 53.18 ± 1.37 μM), and **7q** (IC_{50} = 66.83 ± 1.66 μM) showed poor inhibition towards urease. The *in vitro* urease inhibition values of isatin Schiff base derivatives **7(a-r)** are given in Table 2.

Although all the structural features of any compound mutually contribute to the inhibitory potency, SAR can only be assessed by the changing substituents. In this case, the main changing components are i) $\mathbf{R^1}$ as the hydrazide part, ii) $\mathbf{R^2}$ as the alkyl, allyl and the benzyl substituents and iii) **Y** as the H, NO_2, and Cl substitution on the phenyl ring of the isatin group (Fig. 2). So, it was assumed that these three features are mainly involved in changing the inhibitory potential of the Schiff bases derivatives, *e.g.*, disregarding ibuprofen or mefenamic acid portion, the general trend for the **Y** moiety on the isatin nucleus is NO_2 > H > Cl. The most potent compound in entire series was **7r** having the IC_{50} value 11.36 ± 1.32 μM. This compound exhibited –NO_2 on phenyl ring of isatin moiety as **Y** along with parent Mefenamic acid as R^1, respectively (Fig. 3). On R^2 side it contains only hydrogen atom, thus due to electron withdrawing nature of –NO_2 group, it was suggested it may locate the phenyl ring for better interaction with active site of enzyme. The activity of this compound was compared to the 2nd most active compound of the series **7i** (IC_{50} = 13.38 ± 1.75 μM) of the ibuprofen series. Both of them have the same substitution pattern as R^2 and Y but different R^1 groups. So, in this case the main change was observed by the changing the NSAID drug (R^1). Moreover, compounds **7a** (IC_{50} = 17.37 ± 1.37 μM) and **7j** (IC_{50} = 16.61 ± 1.37 μM) also showed promising inhibitory potential. Through SAR, it was speculated that both also possessed similar features at R^2 and Y but different R^1 groups. The mefenamic acid derivative **7j** was slightly more active than ibuprofen derivative **7a**. The 5th and 6th most active compounds are **7o** (IC_{50} = 18.63 ± 1.27 μM) and **7b** (IC_{50} = 20.56 ± 1.49 μM), exhibiting unsubstituted and chloro isatin with free NH and propyl group as R^2 but different R^1, respectively. On the contrary, if the R^2 is modified from simple NH to N-benzyl or N-butyl in case of compound **7c** (IC_{50} = 36.52 ± 1.33 μM), **7d** (IC_{50} = 33.56 ± 1.52 μM), and **7l** (IC_{50} = 41.17 ± 1.39 μM) the inhibitory potential against urease decreases. Further improvements were observed in **7f** (IC_{50} = 39.18 ± 1.84 μM) and **7 g** (IC_{50} = 45.63 ± 1.73 μM) if we also replaced the H at Y side with Cl group irrespective of which drug was used. The simple isatin derivatives with N-propyl (**7k**, IC_{50} = 59.37 ± 1.59 μM), N-allyl (**7e**, IC_{50} = 60.49 ± 1.53 μM and **7n**, IC_{50} = 76.51 ± 1.48 μM) or N-butyl (**7m**, IC_{50} = 71.25 ± 1.41 μM) substitution, 5-Cl isatin derivatives with N-propyl (**7p**, IC_{50} = 53.18 ± 1.37 μM) and N-benzyl (**7h**, IC_{50} = 68.28 ± 1.16 μM and **7q**, IC_{50} = 66.83 ± 1.66 μM) substitution were found to be less active for this activity. These findings suggest that simple isatin derivatives with no substitution are mainly active in inhibiting urease activity. However, if a sterically hindered bulky group is introduced on the NH of the isatin moiety, activity diminishes. Furthermore, mefenamic acid derivatives are more effective than ibuprofen counterparts in inhibiting the urease activity.

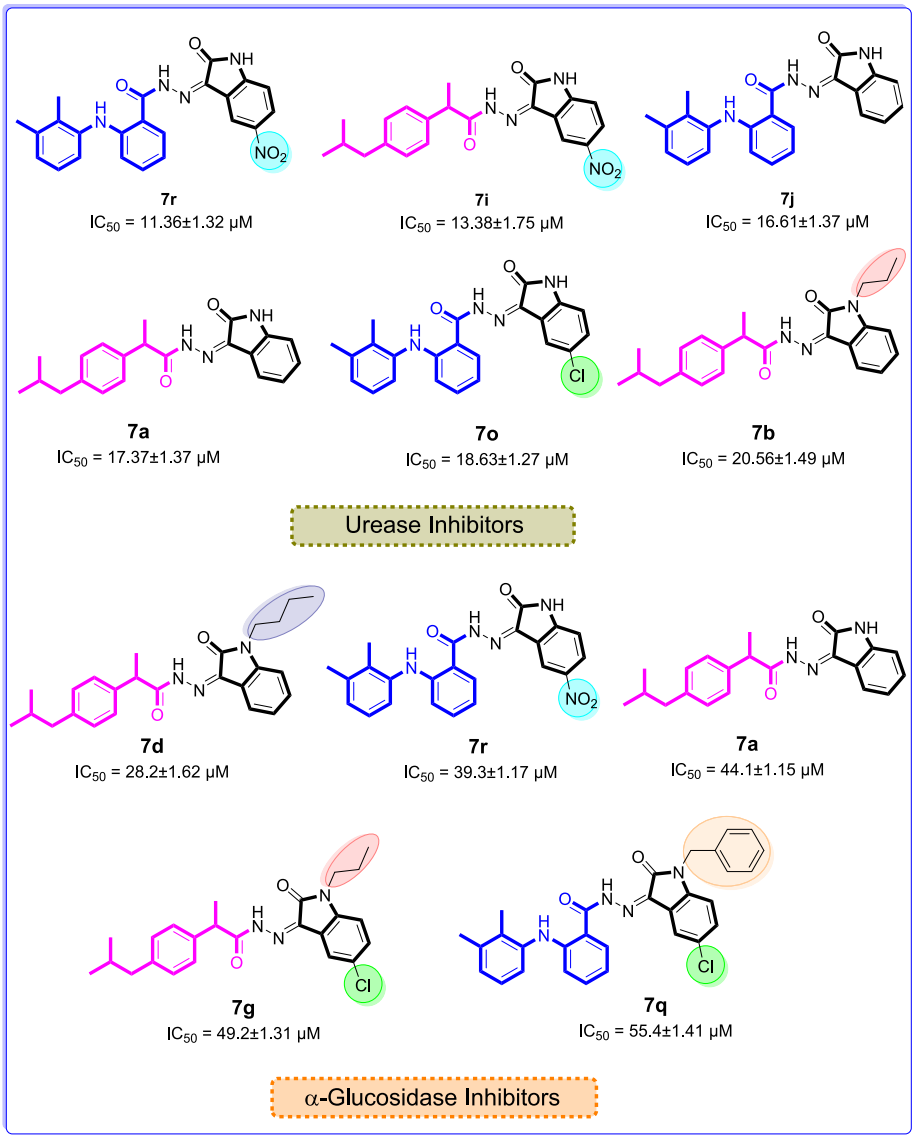

Fig. 3. The most potent inhibitors of urease and α–glucosidase enzymes among the newly synthesized isatin substituted Schiff base derivatives.

3.2.2. α-Glucosidase inhibition and SAR studies

All the target compounds were also screened for their abilities to inhibit α-glucosidase and the results revealed that most of the synthesized derivatives showed promising inhibitory potential between IC_{50} = 28.2 ± 1.62–131.1 ± 1.10 μM than the standard acarbose (IC_{50} value 375.82 ± 1.76 μM), except the compounds **7f**, **7h** and **7i** which were found as moderate inhibitors. Compounds **7b**, **7e** and **7n** were found inactive and the general results are summarized in Table 2. Collectively, mefenamic acid-based compounds (except for **7n**) were equipotent, whereas the activities of ibuprofen-based compounds were strictly dependent on the substitution pattern.

Compound **7d** with IC_{50} value 28.2 ± 1.62 μM is the most potent one among the series. This is the simple isatin derivative containing the ibuprofen portion and exhibiting butyl substitution on R^2 side (Fig. 3). If compared to the mefenamic acid counterpart with the same substituents, the activity decreases up to three folds as clearly observed in compound **7l** having IC_{50} = 97.2 ± 1.19 μM. Compound **7r** (IC_{50} = 39.3 ± 1.17 μM) was the second most active compound, featuring the 5-NO_2 isatin and mefenamic acid as R^1. With the same 5-NO_2 substituent but ibuprofen as R^1, the activity decreases in compound **7i** (IC_{50} = 441.3 ± 1.11 μM) up to 11 folds. The third most active compound in this synthetic library is **7a** (IC_{50} = 44.1 ± 1.15 μM) characterized by the simple isatin and ibuprofen as R^1. Conversely, the corresponding mefenamic acid derivative **7j** (IC_{50} = 81.2 ± 1.33 μM) shows a decrement in activity. The other active compounds belong to the 5-Cl isatin derivatives (**7 g**, IC_{50} = 49.2 ± 1.31 μM and **7q**, IC_{50} = 55.4 ± 1.41 μM). Additionally, these compounds possessed propyl and benzyl substitution on R^2 side, respectively. Contrary to this, the same N-substituents carrying derivatives of mefenamic acid (**7p**, IC_{50} = 60.5 ± 1.53 μM) and ibuprofen (**7h**, IC_{50} = 445.3 ± 2.32 μM) drugs show reduction in their activity.

The simple isatin derivative with the N-propyl substitution shows that the mefenamic acid derivative **7k** (IC_{50} = 66.4 ± 1.41 μM) is more active than the ibuprofen derivative **7b** which was found to be inactive for α–glucosidase enzyme. The same trend is registered for the N-benzyl substituted derivative **7l** (IC_{50} = 97.2 ± 1.19 μM) of mefenamic acid and ibuprofen incorporating derivative **7c** (IC_{50} = 131.1 ± 1.10 μM), as well as the 5-Cl isatin derivatives without any substitution on R^2 side (**7o**, IC_{50} = 70.3 ± 1.14 μM and **7f**, IC_{50} = 397.5 ± 1.12 μM). The N-allyl derivatives (**7e** and **7n**) in both cases were active towards α–glucosidase. It was also observed that the electron-donating groups enhanced the potential of ibuprofen derivatives, whereas electron-withdrawing groups favored the inhibition by mefenamic acid derivatives.

Table 3
Docking score and different type of binding interactions of isatin substituted Schiff base derivatives within the active pocket of urease.

Comp.	Docking Score	Hydrogen bond interactions	Hydrophobic/Other interactions
7r	−6.9236	Asp224 (Conventional H-bond) His222 (Conventional H-bond) Cys322 (2 Conventional H-bonds)	Ni798 (Metal acceptor), Ni799 (Metal acceptor), Ala170 (2 π −alkyl), His323 (2 π − π stacked), Ala366 (π-alkyl), Lys169 (π-alkyl), Lys169 (alkyl-alkyl)
7i	−6.9166	Arg339 (Conventional H-bond)	Asp224 (π-anion), His 323 (π-alkyl), His 323 (alkyl-alkyl), Cys322 (π-σ), Cys322 (alkyl-alkyl), Met367 (alkyl-alkyl), Ala366 (π-alkyl)
7j	−6.7208	Asp224 (2 Conventional H-bonds) Arg339 (Conventional H-bond)	Ala170 (2 π-alkyl), Met367 (alkyl-alkyl), Cys322 (alkyl-alkyl), His323 (π-alkyl), Met318 (alkyl-alkyl)
7a	−6.5107	Glu166 (Conventional H-bond)	Trp225 (π-π T-shaped), Ala170 (2 π-alkyl), Asp224 (π-anion), His323 (π-alkyl), Cys322 (π-σ)
7o	−6.4348	Ala366 (Conventional H-bond) His323 (Carbon H-bond)	His324 (π-π T-shaped), Cys322 (π-sulphur), Ala170 (2 π-alkyl), His222 (π-alkyl), His249 (π-alkyl), His323 (π-alkyl), Cys322 (π-alkyl), Glu166 (π-anion), Lys169 (2 π-alkyl)
7b	−6.0363	Glu166 (Carbon H-bond)	Asp224 (2 π-anion), Ala170 (2 π-alkyl), Cys322 (π-σ), His 323 (π-alkyl), Trp225 (π- π T-shaped)

3.2.3. *Cell viability studies*

All the synthesized derivatives were also biologically evaluated on mononuclear cells (MNCs) isolated from fresh blood. The percentage viability was determined at 0.25 mM concentration (higher than the reported enzymatic inhibition) as mentioned in the experimental section (Table 2), displaying the cellular viability of the synthesized compounds **7(a-r)** between 31.2–95.9 %. The compounds provoking the higher rates of dead cells in this series were **7n** (47.4 %), **7h** (36.8 %), **7e** (31.2 %) and **7f** (41.3 %) did not perform well on inhibition of both enzymes. It also indicates that the most active compounds on urease enzyme, **7a** (69.5 %), **7b** (60.7 %), **7i** (78.9 %), **7j** (72.5 %), **7o** (95.9 %) and **7r** (79.6 %), and against α–glucosidase that is **7d** (55.3 %), **7r** (79.6 %), **7a** (69.5 %), **7g** (59.7 %), and **7q** (77.5 %) were the least cytotoxic. These values are even lesser than the standard cytotoxic drugs Cyclophosphamide, Cisplatin, and Curcumin, a natural reference compound (Table 2). These *in vitro* enzyme inhibition data altogether suggest that isatin-based Schiff base derivatives incorporating ibuprofen and mefenamic acid could significantly inhibit urease and α–glucosidase enzymes, keeping a safe profile towards MNCs.

3.3. *Docking studies*

3.3.1. *Urease inhibitory interactions*

For the molecular docking study, the six most potent derivatives from this series were selected and the results are shown in Table 3. The results were found to be in accordance with the *in vitro* enzyme inhibition studies against urease. Among the derivatives, compound **7r** (IC_{50} = 11.36 ± 1.32 μM) was discovered to be the best-in-class inhibitor, with a docking score of −6.9236. This compound formed four conventional hydrogen bonds with Asp224, His222 and Cys322, two strong metal acceptor interactions with Ni798 and Ni799, and several other interactions. This compound, along with **7i** (IC_{50} = 13.38 ± 1.75 μM, docking score = −6.9166) and **7j** (IC_{50} = 16.61 ± 1.37 μM, docking score = -6.7208), **7a** (IC_{50} = 17.37 ± 1.37 μM, docking score =

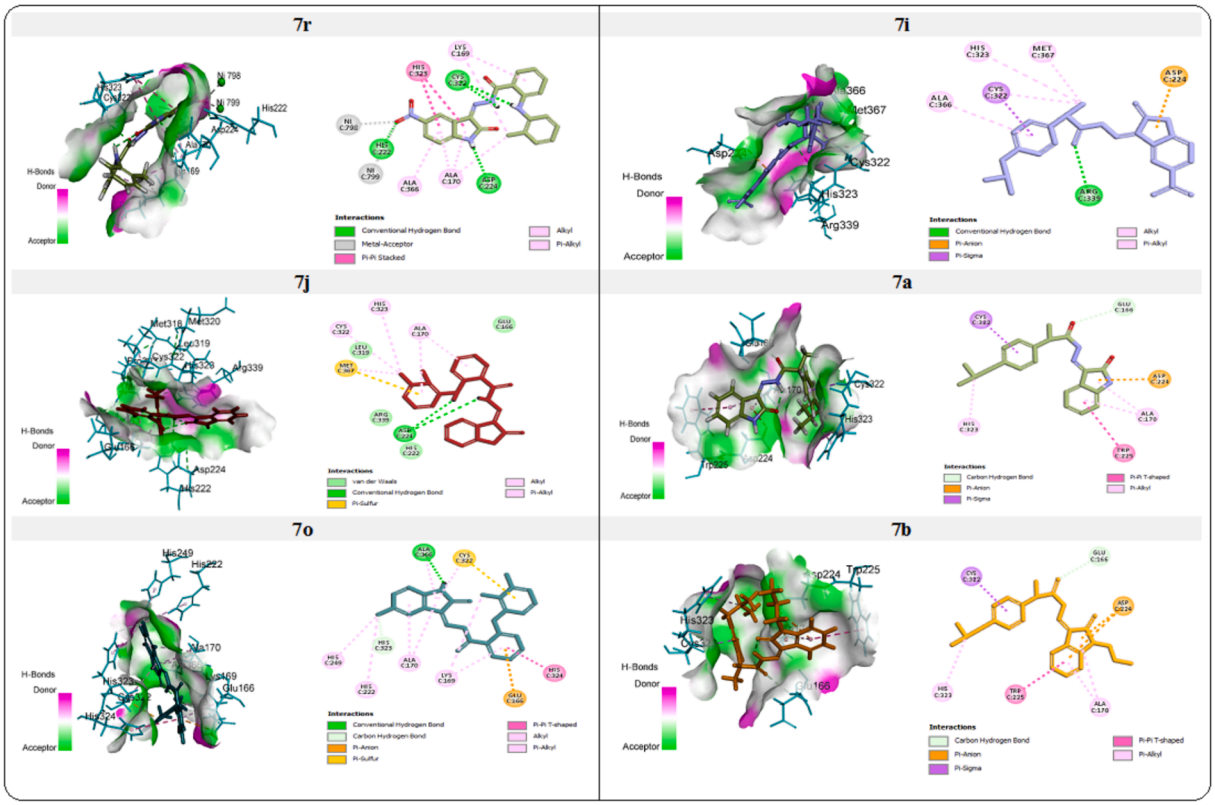

Fig. 4. 3D and 2D interactions of most potent inhibitors within the active pocket of urease.

Table 4
Docking score and different types of binding interactions of isatin substituted Schiff base derivatives within the active pocket of α–glucosidase enzyme.

Comp.	Docking Score	Hydrogen bond interactions	Hydrophobic/Other interactions
7d	−8.5426	Arg315 (C–H-bond)	Phe303 (2 π-π stacked), Arg315 (π-Alkyl), Tyr72 (π-Alkyl)
7r	−8.4093	Asp352 (Conventional H-bond) Gln182 (Conventional H-bond) His112 (2 Conventional H-bonds) His112 (C–H-bond)	Phe314 (2 π-alkyl), Arg315 (π-alkyl), Arg315 (alkyl-alkyl), Tyr158 (π-π T-shaped), Phe178 (π-π T-shaped), Tyr72 (π-π T-shaped)
7a	−8.3641	Tyr158 (Conventional H-bond) Arg315 (pi-donor H-bond)	Phe159 (π-alkyl), Arg442 (alkyl-alkyl), Phe178 (π-alkyl), Arg315 (2 π-alkyl), Tyr158 (π- π T-shaped)
7g	−7.9832	Gln353 (Conventional H-bond) Glu411 (C–H-bond)	His280 (π-alkyl), Arg315 (2 π-alkyl), Arg315 (alkyl-alkyl), Phe159 (π-alkyl), Phe178 (π-alkyl), Tyr158 (π-alkyl)
7q	−7.5620	Gln279 (Conventional H-bond)	Tyr72 (π-alkyl), Phe178 (π-π T-shaped) His351 (2 π-alkyl), Tyr158 (2 π-π T-shaped), Phe314 (π-alkyl), Phe314 (amide π-stacked), Arg315 (π-alkyl), His280 (π-π T-shaped), Val216 (π-alkyl)

−6.5107), **7o** (IC_{50} = 18.63 ± 1.27 μM, docking score = −6.4348), and **7b** (IC_{50} = 20.56 ± 1.49 μM, docking score = −6.0363), established strong hydrogen bond interactions, alkyl-alkyl interactions, π-alkyl interactions, π-π interactions, and several other interactions. Fig. 4 depicts the 2D and 3D interactions.

3.3.2. α-Glucosidase inhibitory interactions

To evaluate the binding interactions, the five most potent derivatives were also chosen for molecular docking studies against this enzyme. The findings were congruent with the *in vitro* enzyme inhibition studies. The docking score of the selected compounds is shown in Table 4. All of the compounds displayed enhanced interactions within the active pocket and were much more effective than acarbose. Among the most active derivatives, compound **7d** (IC_{50} = 28.2 ± 1.62 μM) has been identified as the most potent derivative of α-glucosidase enzyme with a docking score of −8.5426, forming a conventional hydrogen bond with Arg315 through the carbonyl group of the ibuprofen portion. This compound, as well as other potent derivatives *i.e.,* **7r** (IC_{50} = 39.3 ± 1.17 μM, docking score = −8.4093), **7a** (IC_{50} = 44.1 ± 1.15 μM, docking score = −8.3641), **7 g** (IC_5 = 49.2 ± 1.31 μM, docking score = −7.9832), and **7q** (IC_{50} = 55.4 ± 1.41 μM, docking score = −7.5620), formed strong hydrogen bond interactions, alkyl-alkyl interactions, π-alkyl interactions, π-π interactions, and several other interactions. Fig. 5 depicts 3D and 2D binding interactions in the active pocket of α–glucosidase enzyme.

3.4. Prospects of practical applications

Based on the results of the synthesized derivatives, compound **7a** (urease, IC_{50} = 17.37 ± 1.37 μM, α-glucosidase, IC_{50} = 44.1 ± 1.15 μM), **7j**, (urease, IC_{50} = 16.61 ± 1.37 μM and α-glucosidase, IC_{50} = 81.2 ± 1.33 μM), **7o**, (urease, IC_{50} = 18.63 ± 1.27 μM and α-glucosidase, IC_{50} = 70.3 ± 1.14 μM), and **7r** (urease, IC_{50} = 11.36 ± 1.32 μM and α-glucosidase, IC_{50} = 39.3 ± 1.17 μM) had the maximum inhibitory potency against both jack bean urease (thiourea, IC_{50} = 21.37 ± 1.76 μM), and Baker's yeast α-glucosidase (acarbose, IC_{50} = 375.82 ± 1.76 μM) enzyme. As a result, these derivatives **7a**, **7j**, **7o** and **7r** has the ability to block both target enzymes concurrently. Structural optimization, as proposed by molecular docking studies, may improve specificity and effectiveness. Furthermore, the fact that these derivatives are less

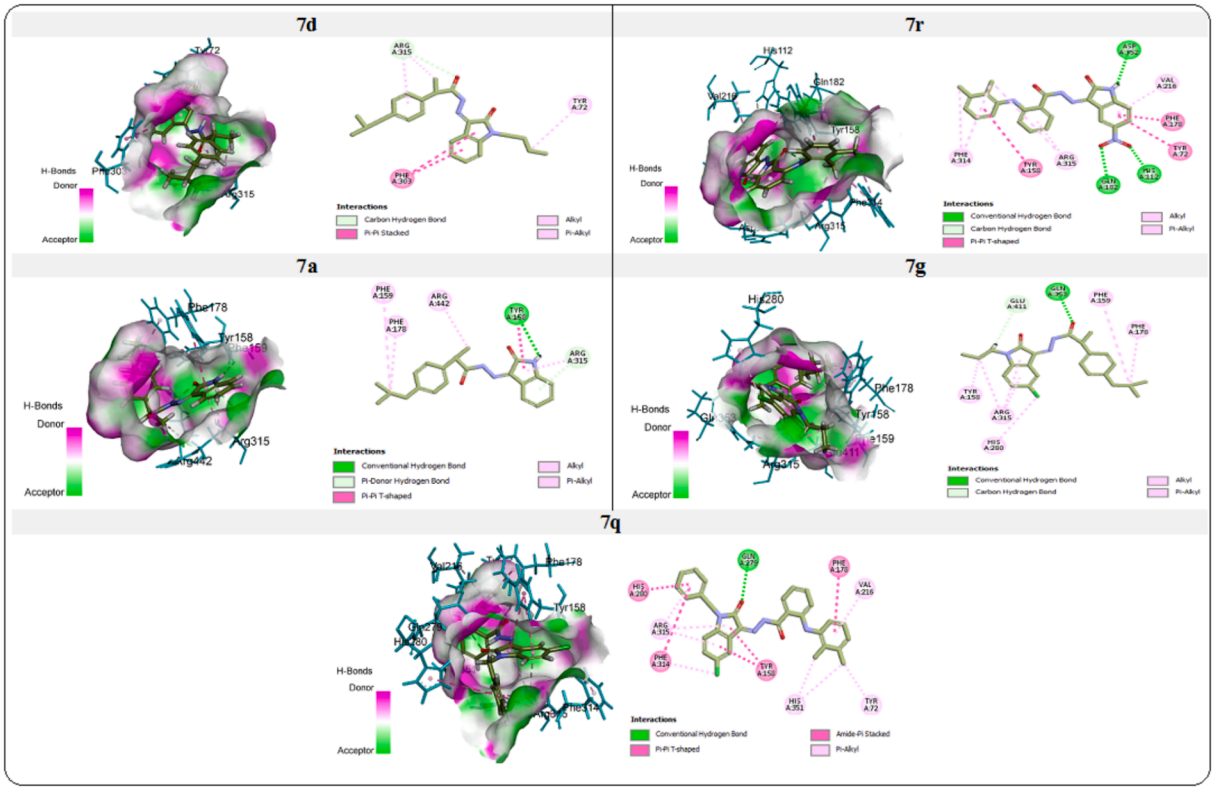

Fig. 5. 3D and 2D interactions of most potent inhibitors within the active pocket of α-glucosidase.

cytotoxic boosts their medicinal potential. The dual inhibitory potency of these derivatives therefore suggested a good option for developing therapies for both diabetes and gastrointestinal diseases simultaneously. The next stages will be to undertake in vivo research, develop better analogues, investigate enzyme inhibition mechanisms, and assess safety and toxicity. These efforts are aimed at developing the leading multi-target inhibitors into a viable therapeutic candidates.

4. Conclusion

In conclusion, we have successfully synthesized a series of 18 Schiff base derivatives incorporating isatin with ibuprofen and mefenamic drugs. These derivatives were also confirmed through spectroscopic (^{1}H NMR & ^{13}C NMR) and HRMS analysis. The biological screening revealed that compounds **7a**, **7j**, **7o** and **7r** displayed dual inhibitory potential towards urease and α–glucosidase enzymes, indicating their potential as a multitarget enzyme inhibitors. These synthesized compounds demonstrated significant enzyme inhibitory activities coupled with low cytotoxicities, showcasing their potential for therapeutic development. Molecular docking studies suggested that structural optimization could enhance their efficacy and specificity. The synthesized derivatives might give a synergistic impact in managing glucose levels and reducing gastrointestinal disorders by concurrently targeting α-glucosidase and urease enzymes, being also characterized by a good cytocompatibility.

Ethical approval

Ethical approval for the use of human blood cells was granted by the animal ethics committee (AEC) of the GC University Faisalabad with an authorization code GCUF/ERC/2178, Research No. 17343, and the IRB (Institution Review Board) No. 343.

CRediT authorship contribution statement

Saima Daud: Writing – original draft, Software, Resources, Methodology, Conceptualization. **Obaid-ur-Rahman Abid:** Supervision, Software, Project administration, Conceptualization. **Malik Saadullah:** Supervision, Project administration, Formal analysis. **M. Fakhar-e-Alam:** Writing – original draft, Software. **Simone Carradori:** Writing – review & editing, Funding acquisition. **Asma Sardar:** Methodology, Investigation, Data curation. **Basit Niaz:** Investigation, Data curation. **M. Atif:** Writing – original draft, Software. **Susi Zara:** Writing – review & editing, Funding acquisition. **Muhammad Rashad:** Writing – original draft, Funding acquisition.

Declaration of competing interest

The authors declare that they have no known competing financial interests or personal relationships that could have appeared to influence the work reported in this paper.

Data availability

Data will be made available on request.

Acknowledgement

This research was supported by PhD fellowship attributed to Rashad Muhammad in the context of MUR National Innovation Ecosystem—Recovery and Resilience Plan (PNRR) Italy and Researchers Supporting Project number (RSP2024R397), King Saud University, Riyadh, Saudi Arabia.

Appendix A. Supplementary material

Supplementary data to this article can be found online at https://doi.org/10.1016/j.jscs.2024.101905.

References

[1] S. Wilt, S. Kodani, T.N.H. Le, et al., Development of multitarget inhibitors for the treatment of pain: design, synthesis, biological evaluation and molecular modeling studies, Bioorg. Chem. 103 (2020) 104165, https://doi.org/10.1016/j.bioorg.2020.104165.
[2] I. Shafique, A. Saeed, A. Ahmed, et al., Exploring the multi-target enzyme inhibition potential of new sulfonamido-thiazoline derivatives; synthesis and computational studies, Results Chem. 4 (2022) 100656, https://doi.org/10.1016/j.rechem.2022.100656.
[3] M. Fan, W. Yang, L. Liu, et al., Design, synthesis, biological evaluation, and docking study of chromone-based phenylhydrazone and benzoylhydrazone derivatives as antidiabetic agents targeting α-glucosidase, Bioorg Chem. 132 (2023) 106384, https://doi.org/10.1016/j.bioorg.2023.106384.
[4] A. Singh, K. Singh, A. Sharma, et al., Recent developments in synthetic α-glucosidase inhibitors: a comprehensive review with structural and molecular insight, J. Mol. Struct. 1281 (2023) 135115, https://doi.org/10.1016/j.molstruc.2023.135115.
[5] M. Saadullah, M. Asif, M. Uzair, et al., Pharmacological evaluation of the hypoglycemic and anti-Alzheimer's activities of aerial parts of Breynia distachia (Phyllanthaceae), Trop. J. Pharm. Res. 21 (2022) 579–587.
[6] M. Saadullah, M. Fakhar-e-Alam, S. Muzammil, et al., Evaluation of molecular mechanisms responsible for in vivo anti-Alzheimer's property of Euphorbia cotinifolia methanol extract, J. King Saud Univ. Sci. 35 (2023) 102785.
[7] M.I. Tousif, S. Tauseef, S. Nabeelah, et al., Phenolics from endophytic fungi as natural α-glucosidase inhibitors: a comprehensive review, J. Mol. Struct. 1291 (2023) 135852, https://doi.org/10.1016/j.molstruc.2023.135852.
[8] V.S. Pawar, D. Bhande, S.D. Pawar, et al., Investigating purification and activity analysis of urease enzyme extracted from jack bean source: a green chemistry approach, Anal. Biochem. 659 (2022) 114925, https://doi.org/10.1016/j.ab.2022.114925.
[9] E. Menteşe, H. Bektaş, B.B. Sokmen, et al., Synthesis and molecular docking study of some 5,6-dichloro-2-cyclopropyl-1H-benzimidazole derivatives bearing triazole, oxadiazole, and imine functionalities as potent inhibitors of urease, Bioorg. Med. Chem. Lett. 27 (2017) 3014–3018, https://doi.org/10.1016/j.bmcl.2017.05.019.
[10] Y. Kayar, Ö. Pamukçu, H. Eroğlu, et al., Relationship between helicobacter pylori infections in diabetic patients and inflammations, metabolic syndrome, and complications, Int. J. Chronic Dis. 2015 (2015) 290128, https://doi.org/10.1155/2015/290128.
[11] J. Vafaeimanesh, M. Parham, M. Seyyedmajidi, et al., Helicobacter pylori infection and insulin resistance in diabetic and nondiabetic population, ScientificWorldJournal 2014 (2014) 391250, https://doi.org/10.1155/2014/391250.
[12] M. Talebi-Taher, M. Mashayekhi, M.H. Hashemi, et al., Helicobacter pylori in diabetic and non-diabetic patients with dyspepsia, Acta Med. Iran. 50 (2012) 315–318.
[13] R. Nath, S. Pathania, G. Grover, et al., Isatin containing heterocycles for different biological activities: analysis of structure activity relationship, J. Mol. Struct. 1222 (2020) 128900, https://doi.org/10.1016/j.molstruc.2020.128900.
[14] S. Ke, L. Shi, Z. Yang, Discovery of novel isatin-dehydroepiandrosterone conjugates as potential anticancer agents, Bioorg. Med. Chem. Lett. 25 (2015) 4628–4631, https://doi.org/10.1016/j.bmcl.2015.08.041.
[15] R. Raju, K. Chidambaram, B. Chandrasekaran, et al., Synthesis, pharmacological evaluation, and molecular modeling studies of novel isatin hybrids as potential anticancer agents, J. Saudi Chem. Soc. 27 (2023) 101598, https://doi.org/10.1016/j.jscs.2023.101598.
[16] L. Emami, S. Khabnadideh, Z. Faghih, et al., Novel N-substituted isatin-ampyrone Schiff bases as a new class of antiproliferative agents: Design, synthesis, molecular modeling and in vitro cytotoxic activity, J. Heterocycl. Chem. 59 (2022) 1144–1159, https://doi.org/10.1002/jhet.4454.
[17] A. Sabt, W.M. Eldehna, T.M. Ibrahim, et al., New antileishmanial quinoline linked isatin derivatives targeting DHFR-TS and PTR1: Design, synthesis, and molecular modeling studies, Eur. J. Med. Chem. 246 (2023) 114959, https://doi.org/10.1016/j.ejmech.2022.114959.
[18] G. Singh, P. Kalra, A. Singh, et al., A quick microwave preparation of isatin hydrazone schiff base conjugated organosilicon compounds: Exploration of their antibacterial, antifungal, and antioxidative potentials, J. Organomet. Chem. 953 (2021) 122051, https://doi.org/10.1016/j.jorganchem.2021.122051.
[19] N. Sin, B.L. Venables, K.D. Combrink, et al., Respiratory syncytial virus fusion inhibitors. Part 7: structure-activity relationships associated with a series of isatin oximes that demonstrate antiviral activity in vivo, Bioorg. Med. Chem. Lett. 19 (2009) 4857–4862, https://doi.org/10.1016/j.bmcl.2009.06.030.
[20] B. Gowrivel Vijayakumar, D. Ramesh, S. Kumari, et al., Enhancing antifungal properties of chitosan by attaching isatin-piperazine-sulfonyl-acetamide pendant groups via novel imidamide linkage, Int. J. Biol. Macromol. 244 (2023) 125428, https://doi.org/10.1016/j.ijbiomac.2023.125428.
[21] A. Kumar, K. Lal, V. Kumar, et al., Synthesis, antimicrobial, antibiofilm and computational studies of isatin-semicarbazone tethered 1,2,3-triazoles, Bioorg. Chem. 133 (2023) 106388, https://doi.org/10.1016/j.bioorg.2023.106388.
[22] A.A. Abu-Hashem, A.B.A. El-Gazzar, H.A.R. Hussein, et al., Synthesis and antimicrobial activity of new triazines, tetrazines, thiazinoquinoxalines, thienotriazepine-imidazo[4, 5-b]quinolines from Isatin derivatives, Polycycl.

Aromat. Compd. 43 (2023) 7073–7092, https://doi.org/10.1080/10406638.2022.2130368.
[23] S.N. Pandeya, D. Sriram, G. Nath, et al., Synthesis, antibacterial, antifungal and anti-HIV evaluation of Schiff and Mannich bases of isatin derivatives with 3-amino-2-methylmercapto quinazolin-4(3H)-one, Pharm Acta Helv. 74 (1999) 11–17, https://doi.org/10.1016/s0031-6865(99)00010-2.
[24] R.K. Thakur, P. Joshi, K. Upadhyaya, et al., Synthesis of isatin based N1-alkylated 3-β-C-glycoconjugated-oxopropylidene oxindoles as potent antiplasmodial agents, Eur. J. Med. Chem. 162 (2019) 448–454, https://doi.org/10.1016/j.ejmech.2018.11.008.
[25] L. Dantas, A.G. Fonseca, J.R. Pereira, et al., Anti-inflammatory and antinociceptive effects of the isatin derivative (Z)-2-(5-chloro-2-oxoindolin-3-ylidene)-N-phenyl-hydrazinecarbothioamide in mice, Braz J. Med. Biol. Res. 53 (2020) e10204.
[26] K. Lahari, R. Sundararajan, Design and synthesis of novel isatin derivatives as potent analgesic, anti-inflammatory and antimicrobial agents, J. Chem. Sci. 132 (2020) 94, https://doi.org/10.1007/s12039-020-01795-0.
[27] L. Manchala, M. Reddy Tatipelly, S. Andole, et al., Synthesis and biological evaluation of new bis isatin derivatives for CNS activity, Mater. Today Proc. 64 (2022) 903–908, https://doi.org/10.1016/j.matpr.2022.06.052.
[28] H. Pervez, N. Khan, J. Iqbal, et al., Synthesis, crystal structure, molecular docking studies and bio-evaluation of some N4-benzyl-substituted isatin- 3-thiosemicarbazones as urease and glycation inhibitors, Heterocycl. Commun. 24 (2018) 51–58, https://doi.org/10.1515/hc-2017-0148.
[29] F. Rahim, M. Taha, N. Iqbal, et al., Isatin based thiosemicarbazide derivatives as potential inhibitor of α-glucosidase, synthesis and their molecular docking study, J. Mol. Struct. 1222 (2020) 128922, https://doi.org/10.1016/j.molstruc.2020.128922.
[30] S. Asirvatham, B.V. Dhokchawle, S.J. Tauro, Quantitative structure activity relationships studies of non-steroidal anti-inflammatory drugs: a review, Arab. J. Chem. 12 (2019) 3948–3962, https://doi.org/10.1016/j.arabjc.2016.03.002.
[31] M.R. Xavier, T.S. Freitas, R.L.S. Pereira, et al., Anti-inflammatory effect, antibiotic potentiating activity against multidrug-resistant strains of Escherichia coli and Staphylococcus aureus, and evaluation of antibiotic resistance mechanisms by the ibuprofen derivative methyl 2-(-4-isobutylphenyl)propanoate, Microb. Pathog. 170 (2022) 105697, https://doi.org/10.1016/j.micpath.2022.105697.
[32] T. Hojatipour, S. Pashapour, A. Almasirad, et al., The cytotoxic activity evaluation of an arylhydrazone derivative of mefenamic acid on HEPG2 liver cancer cells and normal gingival HGF cells, Gene Rep. 33 (2023) 101810, https://doi.org/10.1016/j.genrep.2023.101810.
[33] R. Venkateshwarlu, S. Nath Singh, V. Siddaiah, et al., Ultrasound assisted rapid synthesis of mefenamic acid based indole derivatives under ligand free Cu-catalysis: their pharmacological evaluation, Bioorg. Med. Chem. Lett. 30 (2020) 127112, https://doi.org/10.1016/j.bmcl.2020.127112.
[34] N.H. Naser, A. Abdul Aziz Alibeg, A. Jawad AbdAl-Zahra, Design, synthesis, in silico study and preliminary pharmacological evaluation of ibuprofen derivatives containing 1, 3, 4-Oxadiazole moiety, Mater. Today:. Proc. 65 (2022) 2669–2675, https://doi.org/10.1016/j.matpr.2022.05.092.
[35] R. Ayoub, Q. Jarrar, D. Ali, et al., Synthesis of novel esters of mefenamic acid with pronounced anti-nociceptive effects and a proposed activity on GABA(,) opioid and glutamate receptors, Eur J Pharm Sci. 163 (2021) 105865, https://doi.org/10.1016/j.ejps.2021.105865.
[36] V. Vass, E. Szabó, I. Bereczki, et al., Reperfusion-induced injury and the effects of the dithioacetate type hydrogen sulfide donor ibuprofen derivative, BM-88, in isolated rat hearts, Eur. J. Pharm. Sci. 185 (2023) 106449, https://doi.org/10.1016/j.ejps.2023.106449.
[37] C. Gundogdu-Hizliates, H. Alyuruk, M. Gocmenturk, et al., Synthesis of new ibuprofen derivatives with their in silico and in vitro cyclooxygenase-2 inhibitions, Bioorg. Chem. 52 (2014) 8–15, https://doi.org/10.1016/j.bioorg.2013.10.002.
[38] A.M. Algohary, M.M. Hassan, Novel phospha-oxazepinoquinazolinyl derivatives of ibuprofen as nitric oxide synthase inhibitors: synthesis and biological evaluation, Arab. J. Chem. 15 (2022) 103642, https://doi.org/10.1016/j.arabjc.2021.103642.
[39] D.J. Pérez, M.I. Díaz-Reval, F. Obledo-Benicio, et al., Silicon containing ibuprofen derivatives with antioxidant and anti-inflammatory activities: An in vivo and in silico study, Eur. J. Pharmacol. 814 (2017) 18–27, https://doi.org/10.1016/j.ejphar.2017.07.046.
[40] P. Neeraja, S. Srinivas, K. Mukkanti, et al., 1H–1,2,3-Triazolyl-substituted 1,3,4-oxadiazole derivatives containing structural features of ibuprofen/naproxen: Their synthesis and antibacterial evaluation, Bioorg. Med. Chem. Lett. 26 (2016) 5212–5217, https://doi.org/10.1016/j.bmcl.2016.09.059.
[41] S.I. Farooqi, N. Arshad, P.A. Channar, et al., Synthesis, theoretical, spectroscopic and electrochemical DNA binding investigations of 1, 3, 4-thiadiazole derivatives of ibuprofen and ciprofloxacin: Cancer cell line studies, J. Photochem. Photobiol. B. 189 (2018) 104–118, https://doi.org/10.1016/j.jphotobiol.2018.10.006.
[42] J.K. Savjani, S. Mulamkattil, B. Variya, et al., Molecular docking, synthesis and biological screening of mefenamic acid derivatives as anti-inflammatory agents, Eur. J. Pharmacol. 801 (2017) 28–34, https://doi.org/10.1016/j.ejphar.2017.02.051.
[43] G. Angajala, R. Subashini, V. Aruna, Microwave assisted amberlite-IRA-402 (OH) ion exchange resin catalyzed synthesis of new benzoxazole scaffolds derived from antiinflammatory drugs aceclofenac and mefenamic acid as potential therapeutic agents for inflammation, J. Mol. Struct. 1200 (2020) 127092, https://doi.org/10.1016/j.molstruc.2019.127092.
[44] A.M. Abdulwahid, M.N. Mousa, H.H. Salman, Synthesis and characterization of Some New 1,2,4-Triazole linked to Schiff bases derived from ibuprofen as a possible to inhibit TNF-α Egypt, J. Hosp. Med. 89 (2022) 7314–7320, https://doi.org/10.21608/ejhm.2022.274416.
[45] S. Daud, O.U. Abid, A. Sardar, et al., Exploring ibuprofen derivatives as α-glucosidase and lipoxygenase inhibitors: cytotoxicity and in silico studies, Arch Pharm. (weinheim). 355 (2022) e2200013.
[46] A. Sardar, O.-u.-R. Abid, S. Daud, et al., Identification of novel diclofenac acid and naproxen bearing hydrazones as 15-LOX inhibitors: design, synthesis, in vitro evaluation, cytotoxicity, and in silico studies, Arab. J. Chem. 15 (2022) 104300, https://doi.org/10.1016/j.arabjc.2022.104300.
[47] S. Daud, O.-u.-R. Abid, A. Sardar, et al., Design, synthesis, in vitro evaluation, and docking studies on ibuprofen derived 1,3,4-oxadiazole derivatives as dual α-glucosidase and urease inhibitors, Med. Chem. Res. 31 (2022) 316–336, https://doi.org/10.1007/s00044-021-02814-6.
[48] S. Daud, O.-u.-R. Abid, W. Rehman, et al., In vitro evaluation of novel mefenamic acid derivatives as potential α-glucosidase and urease inhibitors: Design, synthesis, in silico and cytotoxic studies, J. Saudi Chem. Soc. 27 (2023) 101680, https://doi.org/10.1016/j.jscs.2023.101680.
[49] A. Sardar, O.-u.-R. Abid, S. Daud, et al., Design, synthesis, in vitro and in silico studies of naproxen derivatives as dual lipoxygenase and α-glucosidase inhibitors, J. Saudi Chem. Soc. 26 (2022) 101468, https://doi.org/10.1016/j.jscs.2022.101468.
[50] S. Muzaffar, W. Shahid, N. Riaz, et al., Probing phenylcarbamoylazinane-1,2,4-triazole amides derivatives as lipoxygenase inhibitors along with cytotoxic, ADME and molecular docking studies, Bioorg. Chem. 107 (2021) 104525, https://doi.org/10.1016/j.bioorg.2020.104525.
[51] M.W. Weatherburn, Phenol-hypochlorite reaction for determination of ammonia, Anal. Chem. 39 (1967) 971–974, https://doi.org/10.1021/ac60252a045.
[52] M. Fakhar-e-Alam, I. Amjad, M. Saadullah, et al., Antitumor activity of zinc oxide nanoparticles fused with green extract of Nigella sativa, J. Saudi Chem. Soc. 28 (2024) 101814, https://doi.org/10.1016/j.jscs.2024.101814.
[53] A.R. Leach, B.K. Shoichet, C.E. Peishoff, Prediction of protein-ligand interactions. Docking and scoring: successes and gaps, J. Med. Chem. 49 (2006) 5851–5855, https://doi.org/10.1021/jm060999m.
[54] M. Saadullah, A. Farid, A. Ali, et al., Molecular Modeling Study of Novel Lancifolamide Bioactive Molecule as an Inhibitor of Acetylcholinesterase (AChE), Herpes Simplex Virus (HSV-1), and Anti-proliferative Proteins, Molecules 27 (2022), https://doi.org/10.3390/molecules27175480.
[55] M. Liu, W. Zhang, J. Wei, et al., Synthesis and α-glucosidase inhibitory mechanisms of bis(2,3-dibromo-4,5-dihydroxybenzyl) ether, a potential marine bromophenol α-glucosidase inhibitor, Mar Drugs. 9 (2011) 1554–1565, https://doi.org/10.3390/md9091554.
[56] S. Benini, W.R. Rypniewski, K.S. Wilson, et al., The complex of Bacillus pasteurii urease with acetohydroxamate anion from X-ray data at 1.55 Å resolution, JBIC J. Biol. Inorg. Chem. 5 (2000) 110–118, https://doi.org/10.1007/s007750050014.
[57] O.-u.-R. Abid, S. Daud, A. Sardar, et al., Synthesis, urease inhibition screening and molecular docking studies of piperonal based imine derivatives, Med. Chem. Res. 30 (2021) 226–235, https://doi.org/10.1007/s00044-020-02651-z.